ON THE IMPLEMENTATION OF A FINITE-DIFFERENCE COMPUTER CODE FOR THE CALCULATION OF COMPRESSIBLE TRANSONIC/SUPERSONIC VISCOUS FLOWS

João B. P. Falcão Filho – joaobpff@uol.com.br
Centro Técnico Aeroespacial, Instituto de Aeronáutica e Espaço
São José dos Campos –SP – 12228-904
M. A. Ortega – ortega@aer.ita.br
Nide G. C. R. Fico Jr. – nide@aer.ita.br
Instituto Tecnológico de Aeronáutica, Divisão de Engenharia Aeronáutica
São José dos Campos –SP- 12228-900

Abstract: *The ultimate aim of this research effort is the numerical simulation of the turbulent mixing of two parallel jets, one supersonic and the other subsonic, in the presence of a solid wall. The geometry of the flow is two-dimensional. This physical situation is the one to be used as a boostering device in a transonic wind tunnel and has the objective of extending the tunnel's envelope without an excessive increase of the main compressor power. The basics of a finite-difference code, using the implicit Beam and Warming algorithm, is already running including laminar viscous terms. This paper has the objective of reporting the actual status of the study including the validation of the code. The reference problem is a transonic nozzle flow. Special care is taken on the implementation of boundary conditions, especially for the exit section of the nozzle when both supersonic and subsonic regions are already established. Results for the implementation of boundary conditions using zeroth-order extrapolation or the characteristic relations are also reported.*

Key-Words: *Viscous Compressible Flow, Finite-Difference Algorithm, Transonic Nozzle, Mixed Boundary Conditions.*

1. INTRODUCTION

The design and production of the passenger's jet EMB-145 by EMBRAER has placed the Brazilian aeronautical industry in the transonic era. Prior to that, since about the mid-eighties, the Air Ministry has started a coordinated effort in order to equip the Aerospace Technical Center ("Centro Técnico Aeroespacial" - CTA) in São José dos Campos, SP, with a modern transonic testing facility. To this end, the American firm Sverdrup Technology was contracted and the conceptual design of both the tunnel circuit and the pilot circuit were completed with success.

In order to proceed with the transonic wind tunnel project with 70 MW of total power, many theoretical and experimental efforts have been done to get confidence on the technical solutions adopted. The tunnel circuit technology is up to date and incorporates a novel feature: high-enthalpy air injection to extend the tunnel's Reynolds number capability. Injection as the main source of energy to provide flow acceleration is a known practice (Long et al, 1984), but rather, its use as a "boostering" device represents a new technology. As a result of much hard

work, CTA's engineering team has succeeded in designing and building a pilot facility, scaled down 1/8, and the first runs will begin soon. Many theoretical studies were also conducted with the basic aim of understanding the many physical phenomena that happen in a transonic wind tunnel run. Fico Jr. (Fico Jr., 1991, Fico Jr. and Ortega, 1993) obtained curves of flap losses, which hitherto did not exist. Falcão Fo. (1998 and 2000) studied transient phenomena and flow control in the tunnel circuit.

The present paper reports on one more of those theoretical efforts. Specifically, it describes the actual status of the injection process study and the validation of the two-dimensional finite-difference code applied to a transonic nozzle. The implicit Euler method is used for the time march and spatial derivatives are discretized using second order central differences. Standard forth-order artificial dissipation terms are added to the right-hand side of the algorithm while second order ones are used in the left-hand side operators. Several simulations are reported including studies on grid refinement and on the implementation of boundary conditions, especially for the exit section of the nozzle, when both supersonic and subsonic regions are already established. Special attention is dedicated to the implementation of boundary conditions using zeroth-order and characteristic relations to extrapolate data.

The motivation to investigate very carefully the impact of boundary conditions implementation upon the flow at the nozzle exit plane is tied to the next phase of this research effort, the numerical simulation of the turbulent mixing of two parallel jets. Such a mixture occurs, for example, at the injection region of CTA's transonic wind tunnel, which is located at the diffuser entrance. Thus, the subsonic main flow, coming from the second throat, interacts with the supersonic jet emerging from the injector, a small supersonic nozzle. It is clear that meaningful results can only be expected if the flow at the injector exit plane is well established.

2. GOVERNING EQUATIONS AND NUMERICAL IMPLEMENTATION

The non-dimensional Navier-Stokes equations are written in conservation-law form for a two-dimensional, curvilinear coordinate system. Air is considered as a thermal and calorically perfect gas. The governing equations were discretized according to the Beam and Warming (1978) implicit approximate factorization scheme. Time marching was implemented using the implicit Euler method and the spatial derivatives were approximated using central differences. The resulting scheme is second order accurate in space, but only first order accurate in time. However, the aim is to obtain the steady state solutions, therefore, the time evolution of the problem is irrelevant. The details of the equations as well as of their numerical implementation are omitted here because they are very well documented in the literature (Beam and Warming, 1978). For a general treatment of boundary conditions the reader is referred to Hirsch (1988). Other important works closely related to the matter are those of Giles (1990) and Chakravarthy (1983).

2.1 The boundary conditions

A very special emphasis is given here on the implementation of boundary conditions as they play an important role in numerical algorithms. Usually, for internal flows, one has a symmetry boundary that is related to the flow centerline, a wall boundary that is treated according to the mathematical model being used, and an inlet and an outlet boundaries. Special attention will be paid upon the boundary conditions at the entrance and exit planes. Typically, one has to impose the value of certain flow properties at these planes and extrapolate others from the interior of the computational domain. This extrapolation may be done in several ways. In the present work, two approaches are used: a zeroth-order and characteristic relations.

The zeroth-order extrapolation is the simplest of all. It consists in repeating at the desired plane the value of the variables at the interior plane adjacent to it. For example, at the exit

plane, where $i=i_{max}$, variables are set equal to their respective values at the plane $i=i_{max}-1$. On the other hand, the characteristics concept is much more complex and physically sound. It is well known that information is propagated within the fluid along the characteristic lines. The characteristic equations, derived from the Euler equations, which are hyperbolic in nature, can be written as (MacCormack, 1984)

$$\begin{aligned} &\frac{\partial}{\partial t} - \frac{1}{a^2}\frac{\partial p}{\partial t} = -u\left(\frac{\partial}{\partial x} - \frac{1}{a^2}\frac{\partial p}{\partial x}\right), \quad \frac{\partial p}{\partial t} + a\frac{\partial u}{\partial t} = -(u+a)\left(\frac{\partial p}{\partial x} + a\frac{\partial u}{\partial x}\right), \\ &\frac{\partial \mathrm{v}}{\partial t} = -u\frac{\partial \mathrm{v}}{\partial x}, \qquad\qquad\qquad\qquad \frac{\partial p}{\partial t} - a\frac{\partial u}{\partial t} = -(u-a)\left(\frac{\partial p}{\partial x} - a\frac{\partial u}{\partial x}\right), \end{aligned} \tag{1}$$

where the nomenclature is the usual one. The speed of sound is denoted by a and u, u, $(u+a)$ and $(u-a)$ are the eigenvalues associated with the non-viscous Jacobian flux vector in the x-direction. These eigenvalues are related to the direction the information is propagated within the flow. For example, at the inlet plane where the flow is always subsonic the eigenvalues u, u and $(u+a)$ are positive while $(u-a)$ is negative. Thus, in order to have a well-posed problem, one must impose three boundary conditions and extrapolate one from the interior grid points. In the present work the x-component of the velocity vector, u, is extrapolated by one of the two methods described above, while the stagnation pressure, the stagnation temperature and the flow angularity are fixed. At the exit plane, the analysis is not so simple. This is due to the numerical initial conditions. Initially, stagnation properties are set at all grid points except at the exit boundary where the pressure is set as one third of the stagnation pressure. Thus, the flow at the exit plane is initially subsonic and as time progresses it becomes supersonic. Therefore, the treatment of the exit boundary conditions has to be adjusted as the calculation proceeds. In fact, the flow regime at the exit plane must be always checked to determine how many properties should be extrapolated. At a subsonic exit, three values have to be extrapolated from the interior and one is fixed – in this case the outlet static pressure. When the exit flow is supersonic, all four values have to be extrapolated from the interior of the domain. In viscous flow calculations, the presence of the boundary layer represents an extra difficulty because, unlike inviscid flows, one has both supersonic and subsonic regimes at the outlet plane. It is important to realize that inside the boundary layer some points will always stay subsonic. In this respect, the initial pressure assigned to them will be retained until the steady state solution is obtained. This is clearly undesirable, because it is not physically realistic. In order to avoid such an inconvenience several ideas were tested in the present phase of this work.

3. RESULTS

For validation purposes, Euler solutions were considered first. Particularly, inlet boundary conditions were tested. Later laminar viscous flow was calculated and outlet boundary conditions were analyzed.

3.1 The geometry and computational meshes

The geometry considered here, in all cases, is a two-dimensional, transonic convergent-divergent nozzle with the throat located half way between the entrance and exit planes (MacCormack, 1985). The total length of the nozzle is 0.1158 m, the throat height 0.02743 m, the wall radius of curvature at the throat is 0.02743 m and the convergent and divergent

angles are 22.33^o and 1.21^o, respectively. The stagnation temperature, T_t, is equal to 294.8 K while the stagnation pressure, P_t, is 101,360 Pa. Figure 1 shows a typical grid with 21 points in the streamwise direction (ξ direction) and 12 points in the transverse direction (η direction), and 10% stretching. As the geometry is symmetric, only the lower half of the nozzle was considered as the computation domain. All grids were generated algebraically and exponential stretching was implemented for grid refinement near the throat and near the wall.

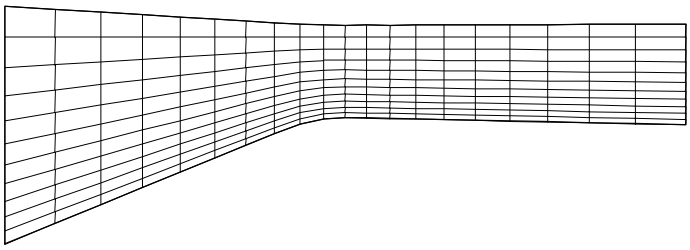

Figure 1 – Grid 21x12, 10% of stretching in both directions.

3.2 Euler formulation.

Figure 2 compares the wall pressure distribution along the nozzle wall, corresponding to an Euler formulation, with experimental results. The grid had 51x40 points. The agreement is very good.

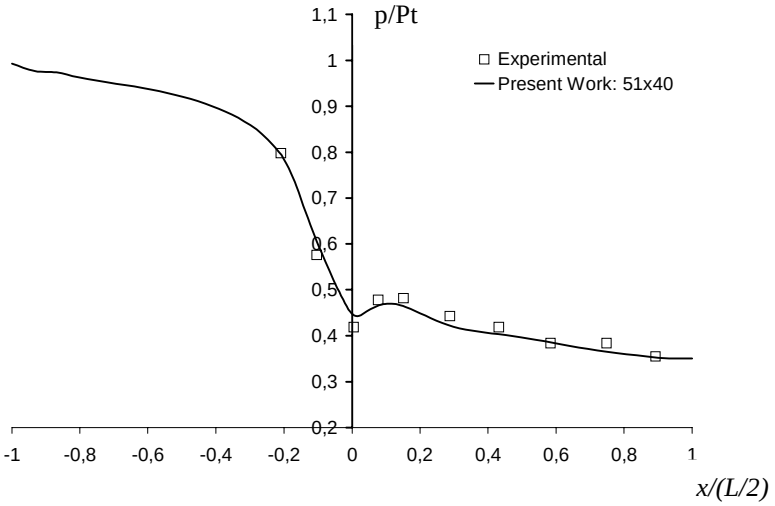

Figure 2 Comparison of results for wall pressure distribution.

For viscous flow simulations, the nozzle geometric values, given in section 3.1, had to be scaled down 100 times in order to assure laminar regime. This downscaled nozzle was simulated again with the Euler version of the code. The grid had 21x12 points. It was observed a small increase of the static pressure at the nozzle entrance. This is due to the position of the wall in respect to the incoming flow angle. This behavior has been observed before (Fico Jr., 1991). Even though the author's main concern here is with the flow quality at the nozzle exit it is wise to investigate if the pressure bump, at the inlet plane, is sensed by the numerical solution at the outlet plane. In order to smooth out the entrance pressure distribution some numerical experiments were done. Three different flow angularities were tested: *(i)* The incoming flow parallel to the nozzle centerline;*(ii)* The incoming flow parallel

to the nozzle wall; *(iii)* Linear variation of angularity from the wall inclination down to zero at the centerline. In all cases, the outlet boundary conditions were extrapolated by characteristics, checking each position at the outlet section grid for supersonic condition. Figures 3 and 4 show the pressure distribution along the wall and along the centerline, respectively, under the three above mentioned assumptions for flow inlet angle. It is apparent that the linear variation yields smoother pressure distributions. More important, in the present context, is the verification that the pressure at exit plane is not affected by the inlet flow angle. Figure 5 shows the pressure distribution field, at the nozzle entrance region, for the three cases analyzed. When the flow entered the nozzle parallel to the centerline the mentioned pressure build up at the wall was observed. On the other hand, when the inlet flow angle was equal to the wall angle the pressure increased at the centerline. However, when linear variation of the inlet angle was imposed, the pressure field became very smooth at the nozzle entrance. The results presented in Figs. 3,4, and 5 corroborate the code validation as the pressure build up region moved at the entrance plane in a very logical way even with a coarse computational mesh.

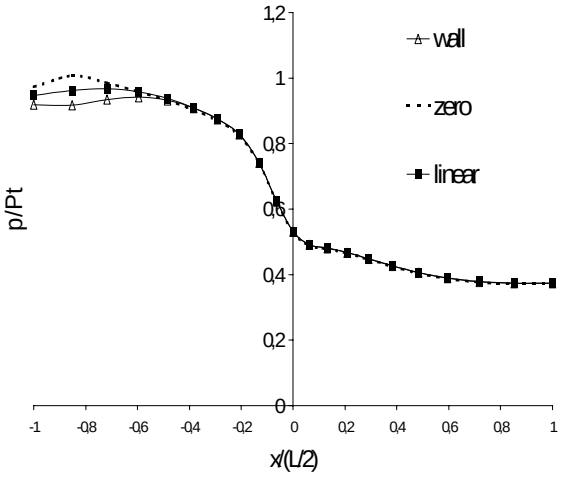

Figure 3 – Wall non-dimensional pressure distribution for inviscid flow, grid 21x12.

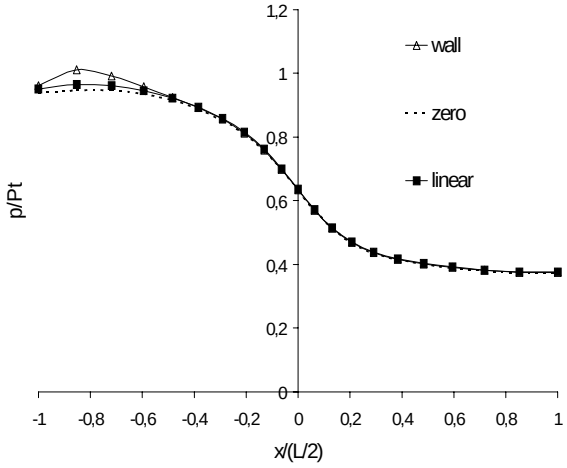

Figure 4 – Centerline non-dimensional pressure distribution for inviscid flow, grid 21x12.

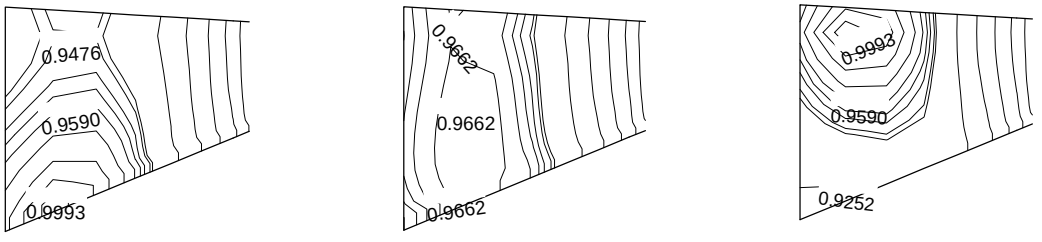

(a) zero inlet flow angle (b) variable inlet flow angle (c) wall inlet flow angle

Figure 5: Isobaric lines at the inlet region for non-viscous flow in a 21x12 grid.

As already mentioned the proper way to treat the exit boundary conditions is related to the sign of the eigenvalues at the outlet plane. In this work, the flow properties are

extrapolated to the outlet grid plane either by zeroth-order extrapolation or by the use of characteristics relations. Down to plot accuracy, the nozzle pressure distributions obtained using either extrapolation techniques are indistinguishable. On the other hand, from data presented in Fig. 6, one can see that the zeroth-order extrapolation enhances the convergence rate. The non-dimensional time step, equal to 0.08, was the same for all cases.

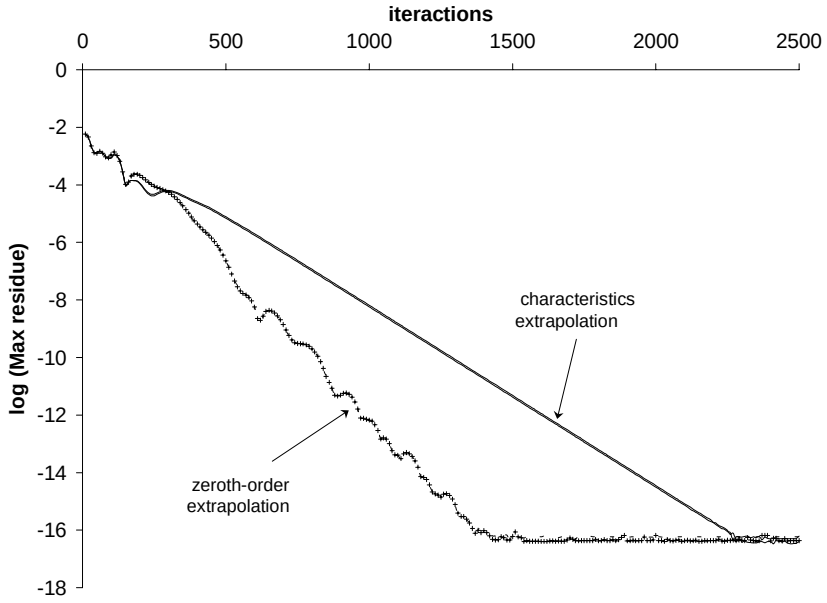

Figure 6 – Convergence history comparison for two kinds of extrapolation.

3.3. Navier-Stokes Solutions

It is important to keep in mind that the motivation here was to search for boundary conditions that would yield realistic flow fields throughout the nozzle and, in particular, at the exit cross section. The reason being that in the next phase of the present research, a mixture of two jets, one of them issuing from nozzle, will be studied.

As mentioned earlier, the characteristics extrapolation scheme is expected to embody "more physics" than the zeroth-order scheme. The viscous formulation brings into the scene the presence of a boundary layer. For this reason, at first, it was decided to check the flow regime at every grid point of the exit boundary. As already mentioned, the original nozzle geometry was scaled down by a factor of 100 to assure laminar flow. The stagnation conditions at the inlet plane are: temperature of 294.8 K, pressure of 101,360 Pa. Thus, the Reynolds number, based on the throat height, is 2,836. The solution maximum residual dropped six orders of magnitude after 1,900 iterations. Figure 7(a) shows the non-dimensional pressure distribution along the nozzle wall for a 21x12 grid. One can observe a sudden change on the curve slope near the exit plane — the last nodes were the most affected. This undesirable behavior is explained by the practice of testing the flow regime at every exit boundary point. This strategy *locks* the pressure at one-third of the stagnation pressure for points for which the flow never turns supersonic. This behavior has no physical meaning. In fact, it brings to the final solution a definite influence of the numerical initial conditions. Should the initial pressure at the nozzle discharge plane be set to a different value, say one forth of the stagnation pressure, the converged solution would be different at the points close to the nozzle wall for which the flow remains subsonic. Further, the anomaly in the pressure distribution is sensed by the velocity profile, as it is evident on Fig. 7(b).

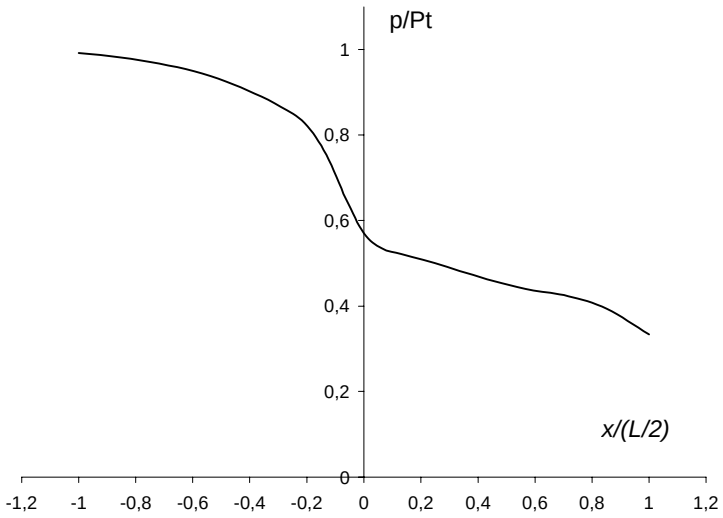

(a) Pressure distribution along nozzle wall.

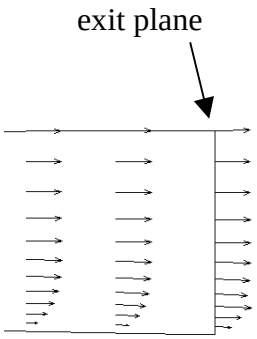

(b)Velocity profiles at nozzle exit region.

Figure 7: Results for Navier-Stokes formulation using a 21x12. Extrapolation by characteristics and flow regime check at all exit points.

The idea of testing the flow regime at every grid point at the exit plane and then apply the "appropriate" boundary condition was not working well. It did not preserve the appropriate physics because it prevents the potential flow to impress the pressure distribution on the boundary layer. Then it was introduced the idea of the flow regime check at the centerline. Thus, a change was introduced in the code, that is, as soon as the point at the centerline experiences the change to supersonic flow the whole exit plane was treated as having supersonic character. The characteristics scheme failed to converge when the check is done at the centerline only. The results are shown in Fig. 8. The pressure distribution at the wall, seen in Fig. 8(a), turned out to be worse than the one shown in Fig 7(a). Figure 8(b) shows how distorted the exit velocity profile became, preventing the numerical solution to converge. The problem here is related to the eigenvalue $\lambda_4 = (u\text{-}a)$. For subsonic flow the information carried by the characteristic line associated to λ_4 travel upstream. Therefore, in these cases the pressure is fixed at the exit boundary. Treating a "subsonic point" as supersonic, one brings into the calculation the eigenvalue (*u-a)* with the *wrong* sign. It should be positive, to carry the information downstream, but in this case, it becomes negative!

Therefore, in this particular situation, the extrapolation using the characteristic equations failed to deliver a smooth solution at the nozzle exit. The next logical try was the combination zeroth-order extrapolation and flow regime testing at the nozzle centerline. All geometrical, physical and numerical parameters remained unchanged. This modification yielded a very smooth steady state solution. Both pressure and velocity profiles presented a behavior that follows well the flow physics, as shown in Fig. 9.

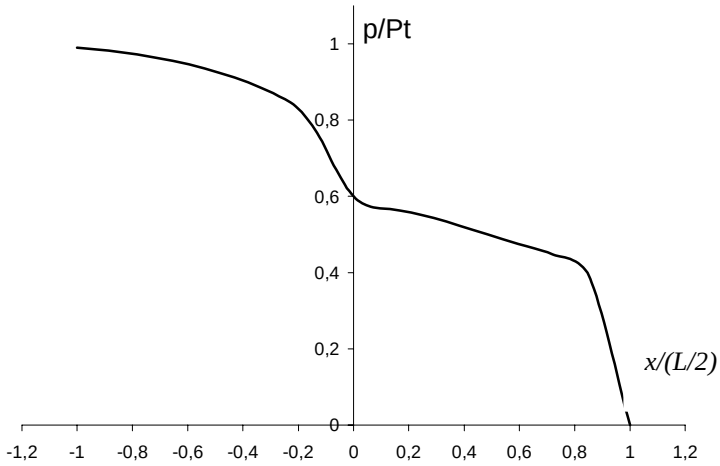

(a) Pressure distribution along the nozzle wall.

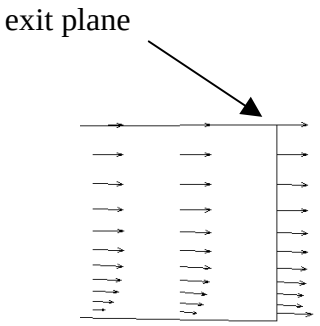

(b) Velocity profiles at nozzle exit region.

Figure 8: Results for Navier-Stokes formulation using a 21x12l grid. Extrapolation by characteristics and flow regime check at the centerline.

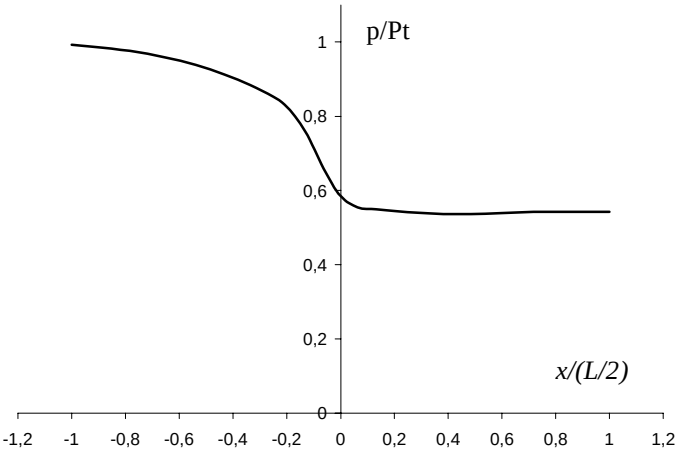

(a) Pressure distribution along the nozzle wall.

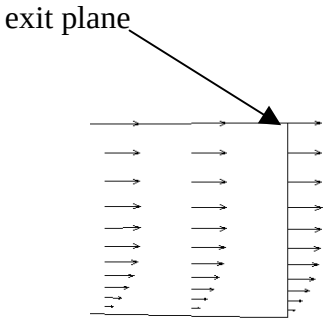

(b)Velocity profiles at nozzle exit region.

Figure 9: Results for Navier-Stokes formulation using a 21x12 grid. Zeroth-order extrapolation and flow regime check at the centerline.

After these preliminary investigations, a systematic study, whose aim was to discover among several possible combinations which one(s) would give a good nozzle solution, was undertaken. By good solution it is meant the one depicted in Fig. 10 – the wall pressure is smooth all along the nozzle and has the right values at the throat and exit sections. Further, the shock at the diverging section is well captured (observe the pressure increase just after the nozzle throat). A summary of all tested cases appears in Table 1. The case was considered converged after the maximum residue dropped six orders of magnitude. As expected convergence became more difficult as the grid was refined. The modifications introduced in the code, represented by cases 4 and 5, were successful in following the physics more closely and therefore enhanced convergence. The main advantage of the zeroth-order extrapolation is

that it has a better convergence rate. It was discovered that three combinations meet the requirements of a good solution: cases 3,4 and 5. The corresponding pressure distributions appear in Fig. 10. Hereafter, their specific features are discussed.

Table 1 – Summary of Navier-Stokes cases. All simulations used $\Delta t = 0.004$.

Case	Flow Regime Check	Extrapolation	Observations	
			Grid 21x12	grid 51x40
1	all points	characteristics	converged	diverged
2	centerline	characteristics	diverged	diverged
3	centerline	zeroth-order	converged	converged
$4^{(1)}$	all points	characteristics	converged	converged
$5^{(2)}$	centerline	characteristics	converged	converged

(1) pressure at subsonic points taken as average of all exit points (2) eingenvalue *(u-a)* taken always positive

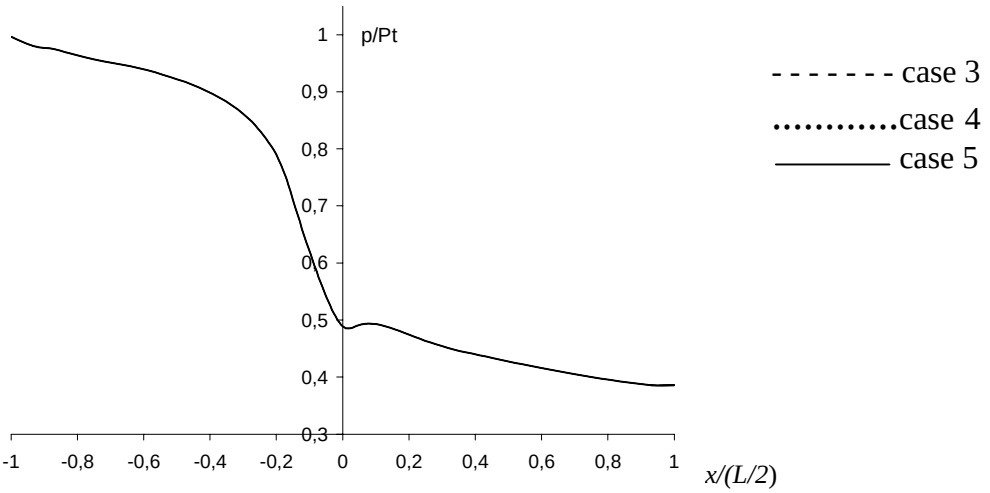

Figure 10: wall pressure distribution for various cases

Case 3, combination centerline/zeroth-order – meaning that subsonic/supersonic regime checking is done only at the centerline and that extrapolation is being done with the zeroth-order scheme – was already mentioned in Fig. 9 relative to a simulation on the coarse 21x12 grid. This is probably the best choice at least for the case in hand. In spite of its "physical lacking" in the extrapolation process, the final result in the refined grid (51x40) is superb. Further, the number of operations is reduced when compared to the other good cases because of the simplicity of the connecting relations.

Case 4, combination of all points/characteristics, incorporates the following strategy: the pressure at the subsonic points was set equal to the average pressure prevailing at exit plane at the previous iteration. This is an attempt to mimic the physical fact that the potential flow outside the boundary layer "impresses" its pressure distribution upon the viscous region. Besides, by doing so one gets rid of the initial value that is set for the static pressure when the point is subsonic.

Case 5, combination centerline/characteristics, is a modification of case 2. Case 2 did not converge on the 21x12 grid. The reason is related to the checking only at the centerline. Once the flow became supersonic at this station, *all* points were treated using the characteristic relations for supersonic flow. This procedure led to numerical overflow, which was related to the sign of the eigenvalue *(u-a)*. Thus, in case 5, after the flow became supersonic at the centerline, only the absolute value of *(u-a)* was considered. Therefore, all information was convected downstream. Physically, this makes sense because the pressure is imposed upon the

boundary layer by the supersonic flow above it and therefore it is dominated by the upstream information.

Another very interesting, and very instructive aspect in terms of validation of the viscous calculation, can be observed by comparing Figs. 2 and 10. One can see that the presence of the boundary layer in the diverging section of the nozzle has two very apparent aspects: the shock is weakened and the exit section pressure is prevented to fall (when compared to non-viscous values). This is a direct effect of the boundary-layer displacement thickness. This displacement corresponds to a smaller transverse section area. With less area, the supersonic expansion effect is lessened and, in consequence, we have the two effects just described.

4. CONCLUSION

The present work investigated the influence of different approaches of boundary conditions implementation upon the numerical solution quality. It was observed that to obtain a smooth pressure field at the entrance plane one should vary the flow angularity of the incoming flow. As for the exit boundary conditions, it was shown that, with proper care, one could choose to enforce it with either zeroth-order or characteristic relations. One should have in mind that at a supersonic exit plane the boundary-layer parabolic character prevents the information to be transmitted upstream.

Acknowledgements

The work of M. A. Ortega was supported in part by the Brazilian agency, National Council of Scientific and Technological Development – CNPq, under grant 522413/96-0.

REFERENCES

- Beam, R.M. and Warming, R.F., 1978, “An Implicit Factored Scheme for the Compressible Navier-Stokes Equations,” *AIAA Journal*, vol. 16, n. 14, pp. 393-402.
- Chakravathy, S.R., 1983, “Euler Equations – Implicit Schemes and Boundary Conditions,” AIAA Journal, 21(5), pp. 699-706.
- Falcão Filho, J.B.P.,Góes L.C.S. and Ortega, M.A., 1998, "Transient Model of the Aerodynamic Circuit of a Transonic Wind Tunnel," Proceedings of the 7th Brazilian Congress of Thermal Sciences, Rio de Janeiro, RJ.
- Falcão Filho, J.B.P.,Góes L.C.S. and Ortega, M.A., 2000, “Prediction of Transients and Control Reactions in a Transonic Wind Tunnel,” Journal of the Brazilian Society of Mechanical Sciences (Accepted for publication).
- Fico, N.G.C.R., Jr., 1991, “Flow Simulation of the Reentry Flap Region in a Transonic Wind Tunnel”, (in Portuguese), Doctor degree thesis, Technological Institute of Aeronautics, São José dos Campos, SP.
- Fico, N.G.C.R, Jr., and Ortega, M. A., 1993, “Numerical Prediction of Flap Losses in a transonic Wind Tunnel,” *AIAA Journal*, Vol. 31, n. 1., pp.133-139.
- Giles, M.B., 1990,“Non Reflecting Boundary Conditions For Euler Equation Calculations, AIAA Journal, 28(12), pp. 2050-2058.
- Hirsch, C., 1988, “Numerical Computation of Internal and External Flows,” John Wiley and Sons, Vol.1 and 2.
- Long, D. F. and Gladen, K. S., 1984, “Development of a Control System for An Injector Powered Transonic Wind Tunnel,” AIAA Paper, pp. 436-445.
- MacCormack, R.W., 1984, “An Introduction and Review of the Basics of Computational Fluid Dynamics”, AIAA Professional Study Series on Computational Fluid Dynamics, Snowmass, Colorado.